in vivo *38*: 321-333 (2024)
doi:10.21873/invivo.13442

Cervical Cytology Preserves Histologically Detected Surface Epithelial Slackening, Unique to the *POLE* Mutation-subtype in Endometrial Cancer

IKUMI KITAZONO[1], TOSHIAKI AKAHANE[2,3], SEIYA YOKOYAMA[3], EMI KUBOTA[1], YUKARI NISHIDA-KIRITA[1], HIROTSUGU NOGUCHI[3], MIKI MURAKAMI[1], SHINTARO YANAZUME[4], HIROAKI KOBAYASHI[4] and AKIHIDE TANIMOTO[2,3,5]

[1]*Department of Surgical Pathology, Kagoshima University Hospital, Kagoshima, Japan;*
[2]*Center for Human Genome and Gene Analysis, Kagoshima University Hospital, Kagoshima, Japan;*
[3]*Department of Pathology, Kagoshima University Graduate School of Medical and Dental Sciences, Kagoshima, Japan;*
[4]*Department of Obstetrics and Gynecology, Kagoshima University Graduate School of Medical and Dental Sciences, Kagoshima, Japan;*
[5]*Center for the Research of Advanced Diagnosis and Therapy of Cancer, Kagoshima University Graduate School of Medical and Dental Sciences, Kagoshima, Japan*

Abstract. *Background/Aim: Among the four genomic subtypes of endometrial cancer, distinguishing between the DNA polymerase epsilon mutation (POLEmut) and no specific molecular profile (NSMP) subtypes requires genomic profiling owing to the lack of surrogate immunohistochemical markers. We have previously found that, histologically, the POLEmut-subtype exhibits surface epithelial slackening (SES). Therefore, to improve subtype identification, we aimed to extract cytological features corresponding to SES in POLEmut-subtype cervical cytology specimens. Materials and Methods: We analyzed 104 endometrial cancer cervical cytology specimens, with integrative diagnosis confirmation via histology, immunohistochemistry, and genomic profiling. Cytological features were evaluated for the presence of atypical glandular cells, atypical cell appearance in single cells and clusters, and cytological SES and the presence of tumor-infiltrating inflammatory cells in clusters. Results: Based on cervical cytology, the POLEmut- and p53mut-subtypes exhibited more frequent atypical cells in smaller clusters, giant tumor cells, and cytological SES patterns than the NSMP-subtype. Tumor-infiltrating lymphocytes were frequent in the POLEmut- and mismatch repair-deficient subtypes. Conclusion: Histologically-detected SES as well as other endometrial cancer features may be preserved in the atypical cell clusters observed in cervical cytology specimens. Cytological detection of SES and of smaller clusters of atypical cells and inflammatory cells with moderate atypia are suggestive of POLEmut-subtype. Integrative diagnosis including genomic profiling remains critical for diagnostic confirmation.*

Correspondence to: Akihide Tanimoto, MD, Ph.D., Department of Pathology, Kagoshima University Graduate School of Medical and Dental Sciences, 8-35-1 Sakuragaoka, Kagoshima 890-8544, Japan. Tel: +81 992755263, Fax: +81 992636348, e-mail: akit09@m3.kufm.kagoshima-u.ac.jp

Key Words: Endometrial cancer, cervical cytology, *POLE*mut-subtype, surface epithelial slackening, genome profiling.

Comprehensive examination of cancer gene alterations is useful for cancer subtype classification, molecularly targeted drug selection, and prognostic speculation (1-3). The Cancer Genome Atlas (TCGA)-based integrative genomic classification system for endometrial tumors, which is introduced in the latest WHO classification of female genital tract tumors (4), includes four subtypes: mismatch repair (MMR)-deficient (MMRd), p53 mutation (p53mut), DNA polymerase epsilon (*POLE*) mutation (*POLE*mut), and no specific molecular profile (NSMP). These categories, which correspond well with prognosis, are helpful in managing patient care in endometrial cancer (5).

MMR and p53 expression provide surrogate markers for diagnosing the MMRd- and p53mut-subtypes, respectively (4, 6). In contrast, because there is no specific antibody for

detecting mutant POLE, genomic examination is essential for differentiating between the *POLE*mut- and NSMP-subtypes. We recently found that the *POLE*mut-subtype often harbors heterozygous *ATM* nonsense mutations, with subsequent loss of ATM expression; nonetheless, ATM immunohistochemistry (IHC) does not provide a complete surrogate marker for diagnosing the *POLE*mut-subtype (7). *POLE*mut-subtype diagnosis therefore requires identification of characteristic histological features such as giant tumor cells (GTCs); however, GTCs are often observed in other subtypes (8, 9). Further, we have recently found that *POLE*mut-subtype endometrial cancers often exhibit a characteristic surface papillary proliferation pattern, which we have named "surface epithelial slackening" (SES). This unique SES pattern, which differs from the hierarchical micropapillary pattern of p53mut-subtype serous carcinoma, was observed in tumor cells facing the uterine lumen (9). Owing to this cell slackening and the ease with which cells detach at the tumor surface facing the uterine lumen, tumor cells may become dissociated from the tumor surface and scatter into cervical cytology specimens. Therefore, we speculate that the histologically detected SES pattern is likely to be reproducible in *POLE*mut-subtype cervical cytology.

To identify cytological features unique to the *POLE*mut-subtype, we compared the cytology of the four endometrial cancer subtypes, confirming the molecular profiling *via* next-generation sequencing (NGS) (10). In the *POLE*mut-subtype cervical cytology, atypical cells frequently formed smaller clusters and exhibited an SES pattern. These features may be characteristic of the *POLE*mut-subtype and hence useful for differentiating it cytologically from the NSMP-subtype.

Materials and Methods

Sample collection. In total, 108 patients with endometrial cancer were registered in the Clinical Research of Cancer Gene Panel Analysis of Gynecologic Cancer Study, conducted between January 2019 and April 2023 at Kagoshima University Hospital, Japan.

Preparation of tissue and cytology specimens, immuno-histochemistry, and next-generation sequencing. The resected tissues were fixed in 10% neutral phosphate-buffered formalin for 24-48 h. The tissues were properly trimmed, processed to prepare formalin-fixed paraffin-embedded (FFPE) specimens, and sectioned for hematoxylin and eosin (H&E) staining, IHC, and next-generation sequencing (NGS). MMR deficiency was defined as the complete loss of nuclear expression of either MLH1 and PMS2, MSH2 and MSH6, MSH6, or PMS2 alone. Diffuse and strong nuclear expression or complete loss of p53 expression were defined as the mutation patterns. Scattered nuclear staining with variable p53 expression intensity was categorized as the wildtype pattern. All antibodies used for IHC analysis were purchased from DAKO (Glostrup, Denmark). The cytological specimens were processed using conventional smear or liquid-based cytology (LBC). To prepare LBC specimens, cervical cytology specimens were immediately fixed with CytoRich Red solution (Becton Dickinson, Franklin Lakes, NJ, USA). The cytology slides were then processed using a BD SurePath liquid-based Pap Test System (Becton Dickinson) and stained with Papanicolaou staining solution.

Genome analysis and integrative diagnosis. Genomic profiles were examined using a custom NGS gene panel as previously reported (9-11). The Gynecologic Cancer Panel Ver. 2 (Qiagen, Hilden, Germany), containing 56 cancer-related genes and 17 microsatellite regions, was used for NGS analysis to determine gene alterations, tumor mutation burden, and microsatellite instability, as previously reported (9-11). After DNA was obtained from the FFPE sections (10-μm thickness) representing ≥30% of the cancerous tissue area, NGS was performed using a MiSeq sequencer (Illumina, San Diego, CA, USA). No fresh frozen or normal tissue were used for the study. The sequence data were annotated using the Qiagen web portal (https://www.qiagen.com./us/shop/genes-and-pathways/data-analysis-center-overview-page/) and Mitsubishi Electronic Software (Amagasaki, Hyogo, Japan) (12) using reference data from the COSMIC database (v.90.0; https://cancer.sanger.ac.uk/cosmic) and the reference human genome GRCh37/hg19 (https://www.ncbi.nlm.nih.gov/assembly/GCF_000001405.13/). The sequence data obtained from whole blood DNA were used only as a reference, and germline analysis was not performed. Integrated pathological diagnoses were made according to the WHO and TCGA classification systems (4, 5) by two board-certified surgical and molecular pathologists (IK and AT). TNM clinical classification was performed according to the Union for International Cancer Control (UICC) system (13).

Evaluation of cytology specimens. Cervical cytological features were classified as negative for intraepithelial lesion or malignancy (NILM), or as having atypical glandular cells (AGC), AGC-favor neoplastic cells, or as adenocarcinoma cells, according to the Bethesda System (14). Atypical or adenocarcinoma cells were classified based on their dominant grouping (small or large clusters, or single cells). Clusters were considered large with >20 atypical cells or small with ≤20 atypical cells. The category comprising >50% of the combined clusters and single cells was selected as the dominant category for that sample. We detected the presence or absence in the clusters of tumor infiltrating lymphocytes (TILs) and tumor-infiltrating neutrophils (TINs).

Cytologically, SES was identified in atypical cell clusters based on the loosening or detachment of individual cells from the cell cluster periphery. An SES-positive cluster was defined as one exhibiting cellular loosening or dissociation in ≥50% of the cluster perimeter. Clusters exhibiting cytologically detected SES (cSES) was counted. The presence or absence of GTCs was determined.

Statistical analysis. Statistical comparisons were performed using Kruskal-Wallis, Wilcoxon, and Fisher's exact tests. Differences were considered statistically significant at $p<0.05$ and borderline significant at $p<0.1$. The cSES count was evaluated using a receiver operator characteristic (ROC) curve.

Ethical approval. The use of the clinical samples was approved by the Ethics Committee for Clinical and Epidemiologic Research of Kagoshima University (approval no. 180215) and the 1964 Helsinki Declaration, including its later amendments and comparable ethical standards. Written informed consent was obtained from all the

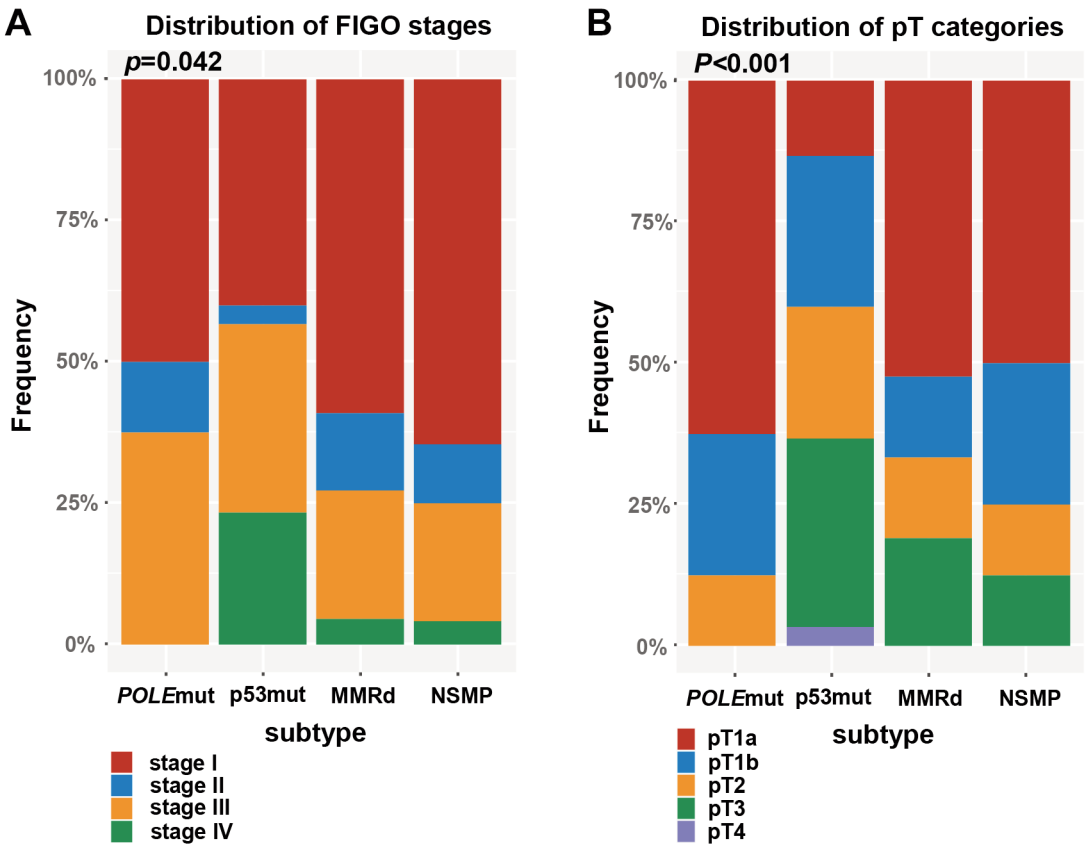

Figure 1. *Endometrial cancer subtype clinical stages. (A) Based on the International Federation of gynecology and Obstetrics (FIGO) stage distribution, FIGO stage is significantly different among the subtypes (Kruskal-Wallis test): the p53mut-subtype exhibits significantly more-advanced stages on admission (Fisher's exact test) (Table II). (B) Pathological T (pT) category frequency is significantly different among the subtypes (Kruskal-Wallis test). MMRd, Mismatch repair-deficient; NSMP, no specific molecular profile; p53mut, p53 mutation; POLEmut, DNA polymerase epsilon mutation.*

participants prior to the study. Participants younger than 20 years of age were excluded.

Results

Clinical summary. Among the 108 registered endometrial cancer cases, 103 were available for evaluation *via* cervical cytology and were included here. Table I presents the clinical findings, staging, and pathological diagnoses of these 103 cases, among these, there were eight *POLE*mut-, 22 MMRd, 28 p53mut-, and 45 NSMP subtypes cases. The *POLE*mut-subtype was observed in endometrioid carcinomas and mixed carcinomas (those with components of endometrioid and clear cell carcinomas). The MMRd-subtype was observed in endometrioid carcinomas, dedifferentiated carcinomas, serous carcinomas, carcinosarcomas, and clear cell carcinomas. Most of the p53mut-subtpye cases were serous carcinomas or carcinosarcomas. Most of the NSMP-subtype cases were endometrioid carcinomas.

The UICC-based International Federation of Gynecology and Obstetrics (FIGO)-stage (2008) distribution varied significantly among the four subtypes (Figure 1A): the p53mut-subtype exhibited more-advanced FIGO stages than the MMRd- and NSMP-subtypes (Table II). UICC pathological T category frequencies showed a significant difference among the four subtypes (Figure 1B): the p53mut-subtype exhibited more-advanced pathological T categories than the NSMP-subtypes (Table II).

Cervical cytology of POLEmut-subtype endometrial cancer. Abnormal cervical cytology, including atypical or adenocarcinoma cells, was observed in 55-75% of specimens. The *POLE*mut-subtype appeared predominantly as small clusters or as single atypical cells with moderate nuclear atypia (Figure 2A). Most clusters exhibited cell dissociation around the entire circumference of the clusters, forming the cSES pattern (Figure 2B and C). Many of the clusters contained inflammatory cells (TILs, TINs, or both).

Table I. *Clinical, pathological, and cytological summaries*.

Case no.	Age	Histological diagnosis	Molecular subtypes	pT	FIGO Stage*	Type of cytology sample	Cytomorphologic features					
							Abnormal cytology	Cluster size	SES count	TIN	TIL	GTC
1	57	Endometrioid carcinoma, G1	*POLE*mut	pT1a	Stage I	Conv.	ca(+)	Large	3	(+)	(+)	(–)
2	54	Endometrioid carcinoma, G2	*POLE*mut	pT1a	Stage I	Conv.	NILM	ne				
3	62	Mixed carcinoma (CCC and ECG1)	*POLE*mut	pT1b	Stage III	Conv.	ca(s/o)	Small	7	(+)	(+)	(+)
4	55	Endometrioid carcinoma, G2	*POLE*mut	pT1a	Stage III	Conv.	NILM	ne				
5	53	Endometrioid carcinoma, G2	*POLE*mut	pT1a	Stage III	LBC	ca(+)	Small	15	(–)	(+)	(+)
6	59	Endometrioid carcinoma, G3	*POLE*mut	pT1b	Stage I	LBC	ca(+)	Single	4	(+)	(+)	(+)
7	34	Endometrioid carcinoma, G1	*POLE*mut	pT1a	Stage I	LBC	AGC	Small	4	(–)	(+)	(–)
8	55	Mixed carcinoma (CCC and ECG2)	*POLE*mut	pT2	Stage II	LBC	ca(+)	Small	1	(+)	(–)	(–)
9	51	Dedifferentiated carcinoma	MMRd	pT1a	Stage III	Conv.	AGC	Single	0	(–)	(–)	(–)
10	57	Dedifferentiated carcinoma	MMRd	pT3	Stage III	Conv.	ca(s/o)	Small	0	(+)	(–)	(+)
11	71	Dedifferentiated carcinoma	MMRd	pT3	Stage III	Conv.	NILM	ne				
12	72	Serous carcinoma	MMRd	pT1a	Stage I	Conv.	ca(+)	Small	5	(+)	(+)	(+)
13	68	Endometrioid carcinoma, G2	MMRd	pT2	Stage II	Conv.	AGC	Large	0	(+)	(+)	(–)
14	64	Endometrioid carcinoma, G3	MMRd	na	Stage IV	Conv.	NILM	ne				
15	59	Endometrioid carcinoma, G2	MMRd	pT2	Stage II	Conv.	AGC	Small	0	(+)	(+)	(–)
16	60	Endometrioid carcinoma, G1	MMRd	pT1a	Stage I	Conv.	ca(+)	Large	1	(+)	(+)	(–)
17	52	Carcinosarcoma	MMRd	pT2	Stage II	Conv.	AGC	Large	0	(+)	(+)	(–)
18	78	Endometrioid carcinoma, G3	MMRd	pT1a	Stage I	Conv.	NILM	ne				
19	58	Endometrioid carcinoma, G1	MMRd	pT1a	Stage I	LBC	AGC	Small	3	(+)	(–)	(–)
20	66	Endometrioid carcinoma, G1	MMRd	pT1b	Stage I	Conv.	NILM	ne				
21	49	Endometrioid carcinoma, G1	MMRd	pT3	Stage III	LBC	NILM	ne				
22	60	Carcinosarcoma	MMRd	pT1b	Stage I	LBC	NILM	ne				
23	58	Endometrioid carcinoma, G2	MMRd	pT1a	Stage I	LBC	ca(+)	Small	4	(+)	(+)	(+)
24	56	Endometrioid carcinoma, G2	MMRd	pT1a	Stage I	LBC	NILM	ne				
25	58	Endometrioid carcinoma, G1	MMRd	pT1a	Stage I	LBC	NILM	ne				
26	58	Endometrioid carcinoma, G1	MMRd	pT1a	Stage I	LBC	ca(+)	Small	3	(+)	(+)	(–)
27	49	Endometrioid carcinoma, G1	MMRd	pT1a	Stage I	LBC	ca(+)	Large	0	(+)	(+)	(–)
28	67	Endometrioid carcinoma, G1	MMRd	pT1a	Stage I	LBC	AGC	Large	1	(–)	(+)	(–)
29	79	Endometrioid carcinoma, G1	MMRd	pT1b	Stage I	LBC	NILM	ne				
30	57	Endometrioid carcinoma, G3	MMRd	pT3	Stage III	LBC	NILM	ne				
31	80	Carcinosarcoma	p53mut	pT3	Stage III	Conv.	ca(+)	Small	4	(+)	(+)	(+)
32	64	Serous carcinoma	p53mut	pT3	Stage IV	Conv.	ca(+)	Large	0	(+)	(–)	(–)
33	78	Mixed carcinoma (SC and ECG1)	p53mut	pT1a	Stage IV	Conv.	ca(+)	Small	0	(+)	(+)	(+)
34	67	Serous carcinoma	p53mut	pT3a	Stage III	Conv.	ca(s/o)	Small	4	(+)	(+)	(+)
35	57	Serous carcinoma	p53mut	pT1a	Stage I	Conv.	NILM	ne				
36	63	Serous carcinoma	p53mut	pT2	Stage III	Conv.	AGC	Small	0	(+)	(–)	(–)
37	75	Serous carcinoma	p53mut	pT1b	Stage I	Conv.	AGC	Small	3	(+)	(+)	(–)
38	59	Endometrioid carcinoma, G1	p53mut	pT1b	Stage I	na						
39	56	SEIC	p53mut	pT1b	Stage I	Conv.	AGC	Small	0	(–)	(–)	(–)
40	70	Serous carcinoma	p53mut	pT1b	Stage III	Conv.	NILM	ne				
41	58	Carcinosarcoma	p53mut	pT4	Stage IV	Conv.	ca(+)	Single	0	(–)	(+)	(+)
42	65	Serous carcinoma	p53mut	pT1b	Stage I	Conv.	ca(+)	Small	0	(+)	(–)	(–)
43	67	Serous carcinoma	p53mut	pT1b	Stage III	Conv.	NILM	ne				
44	77	Serous carcinoma	p53mut	pT1b	Stage I	Conv.	NILM	ne				
45	63	Adenocarcinoma/CCC	p53mut	pT1b	Stage IV	Conv.	NILM	ne				
46	72	Dedifferentiated carcinoma	p53mut	pT3	Stage III	Conv.	ca(+)	Small	10	(+)	(–)	(+)
47	63	Neuroendocrine carcinoma	p53mut	pT3	Stage III	LBC	ca(+)	Small	3	(–)	(–)	(+)
48	75	Serous carcinoma	p53mut	pT3	Stage III	LBC	ca(+)	Small	20	(–)	(–)	(+)
49	60	Serous carcinoma	p53mut	pT3	Stage IV	Conv.	NILM					
50	59	Endometrioid carcinoma, G2	p53mut	pT3	Stage III	LBC	ca(+)	Small	0	(+)	(–)	(–)
51	55	Endometrioid carcinoma, G3	p53mut	pT1a	Stage I	LBC	NILM	ne				
52	88	Neuroendocrine carcinoma	p53mut	pT3	Stage III	na						
53	57	Endometrioid carcinoma, G2	p53mut	pT1a	Stage IV	LBC	ca(+)	Small	4	(–)	(–)	(–)
54	62	Clear cell carcinoma	p53mut	pT3	Stage IV	LBC	NILM	ne				
55	72	Endometrioid carcinoma, G1	p53mut	pT2	Stage II	LBC	ca(+)	Large	0	(+)	(+)	(–)

Table I. *Continued*

Table I. *Continued*

Case no.	Age	Histological diagnosis	Molecular subtypes	pT	FIGO Stage*	Type of cytology sample	Cytomorphologic features					
							Abnormal cytology	Cluster size	SES count	TIN	TIL	GTC
56	68	Endometrioid carcinoma, G3	p53mut	pT2	Stage I	LBC	NILM	ne				
57	54	Serous carcinoma	p53mut	pT2	Stage I	LBC	NILM	ne				
58	58	Carcinosarcoma	p53mut	pT2	Stage I	LBC	NILM	ne				
59	77	Carcinosarcoma	p53mut	pT2	Stage I	LBC	AGC	Small	1	(+)	(+)	(+)
60	75	SEIC	p53mut	pT2	Stage I	LBC	ca(+)	Small	0	(+)	(+)	(+)
61	61	Endometrioid carcinoma, G1	NSMP	pT1a	Stage I	Conv.	AGC	Small	0	(–)	(–)	(–)
62	60	Endometrioid carcinoma, G2	NSMP	pT2	Stage II	Conv.	AGC	Large	0	(+)	(–)	(–)
63	39	Endometrioid carcinoma, G1	NSMP	pT1a	Stage I	Conv.	ca(+)	Small	0	(–)	(–)	(–)
64	59	Endometrioid carcinoma, G1	NSMP	pT3	Stage III	Conv.	NILM	ne				
65	75	Squamous cell carcinoma	NSMP	pT1a	Stage I	Conv.	AGC	Large	0	(+)	(–)	(–)
66	71	Endometrioid carcinoma, G1	NSMP	pT1b	Stage I	Conv.	ca(s/o)	Small	4	(+)	(–)	(–)
67	63	Carcinosarcoma	NSMP	pT3	Stage III	Conv.	AGC	Large	0	(–)	(–)	(–)
68	58	Clear cell carcinoma	NSMP	pT2	Stage IV	Conv.	ca(+)	Small	0	(+)	(–)	(+)
69	52	Endometrioid carcinoma, G1	NSMP	pT1a	Stage I	Conv.	NILM	ne				
70	43	Endometrioid carcinoma, G1	NSMP	pT1a	Stage I	Conv.	NILM	ne				
71	65	Endometrioid carcinoma, G2	NSMP	pT1b	Stage I	Conv.	NILM	ne				
72	67	Endometrioid carcinoma, G2	NSMP	pT3	Stage III	Conv.	AGC	Large	1	(+)	(+)	(+)
73	84	Clear cell carcinoma	NSMP	pT1a	Stage I	Conv.	AGC	Single	0	(–)	(–)	(–)
74	42	Endometrioid carcinoma, G1	NSMP	pT1a	Stage I	na						
75	63	Endometrioid carcinoma, G1	NSMP	pT1a	Stage I	Conv.	AGC	Large	0	(+)	(–)	(–)
76	61	Endometrioid carcinoma, G1	NSMP	pT1a	Stage I	LBC	AGC	Large	0	(+)	(–)	(–)
77	63	Endometrioid carcinoma, G2	NSMP	pT1a	Stage I	Conv.	NILM	ne				
78	47	Endometrioid carcinoma, G1	NSMP	pT1b	Stage I	Conv.	NILM	ne				
79	56	Endometrioid carcinoma, G1	NSMP	pT1b	Stage I	na						
80	55	Endometrioid carcinoma, G2	NSMP	pT3	Stage III	Conv.	ca(s/o)	Large	0	(–)	(–)	(–)
81	56	Endometrioid carcinoma, G1	NSMP	T1a	Stage IV	Conv.	AGC	Large	1	(+)	(+)	(–)
82	53	Endometrioid carcinoma, G1	NSMP	pT2	Stage II	Conv.	ca(+)	Large	2	(–)	(–)	(–)
83	61	Endometrioid carcinoma, G1	NSMP	pT2	Stage II	Conv.	ca(+)	Large	0	(–)	(–)	(–)
84	61	Endometrioid carcinoma, G2	NSMP	pT1b	Stage I	LBC	NILM	ne				
85	75	Mucinous carcinoma	NSMP	pT1a	Stage I	LBC	ca(+)	Small	0	(–)	(–)	(–)
86	49	Endometrioid carcinoma, G1	NSMP	pT1a	Stage I	LBC	AGC	Small	1	(+)	(–)	(–)
87	60	Endometrioid carcinoma, G2	NSMP	pT1a	Stage I	LBC	ca(+)	Large	0	(–)	(–)	(–)
88	68	Endometrioid carcinoma, G2	NSMP	pT1a	Stage I	LBC	AGC	Large	0	(+)	(+)	(–)
89	63	Endometrioid carcinoma, G2	NSMP	pT1a	Stage I	LBC	NILM	ne				
90	73	Endometrioid carcinoma, G2	NSMP	pT1b	Stage I	LBC	NILM	ne				
91	53	Endometrioid carcinoma, G1	NSMP	pT1a	Stage I	LBC	NILM	ne				
92	52	Endometrioid carcinoma, G1	NSMP	pT1a	Stage I	LBC	NILM	ne				
93	59	Endometrioid carcinoma, G1	NSMP	pT1b	Stage III	LBC	NILM	ne				
94	46	Endometrioid carcinoma, G1	NSMP	pT1a	Stage I	LBC	AGC	Large	0	(+)	(+)	(–)
95	91	Endometrioid carcinoma, G1	NSMP	pT2	Stage II	LBC	NILM	ne				
96	64	Endometrioid carcinoma, G2	NSMP	pT1b	Stage III	LBC	NILM	ne				
97	61	Endometrioid carcinoma, G1	NSMP	pT1b	Stage III	LBC	ca(+)	Large	0	(+)	(–)	(–)
98	28	Endometrioid carcinoma, G1	NSMP	pT1a	Stage I	LBC	AGC	Large	0	(–)	(–)	(–)
99	40	Endometrioid carcinoma, G1	NSMP	pT1a	Stage I	LBC	NILM	ne				
100	49	Endometrioid carcinoma, G1	NSMP	pT1b	Stage I	na						
101	66	Endometrioid carcinoma, G1	NSMP	pT1b	Stage III	LBC	ca(+)	Small	1	(–)	(–)	(–)
102	51	Endometrioid carcinoma, G1	NSMP	pT1a	Stage I	LBC	NILM	ne				
103	47	Endometrioid carcinoma, G1	NSMP	pT1a	Stage I	LBC	AGC	Small	0	(–)	(+)	(–)
104	38	Endometrioid carcinoma, G1	NSMP	pT3	Stage III	LBC	NILM	ne				
105	42	Endometrioid carcinoma, G1	NSMP	pT1a	Stage I	LBC	AGC	Small	2	(+)	(–)	(–)
106	66	Endometrioid carcinoma, G1	NSMP	pT1a	Stage I	LBC	NILM	ne				
107	56	Endometrioid carcinoma, G1	NSMP	pT2	Stage II	LBC	ca(+)	Large	0	(+)	(+)	(–)
108	49	Endometrioid carcinoma, G2	NSMP	pT3	Stage III	LBC	ca(+)	Small	0	(+)	(+)	(–)

SES, Surface epithelial slackening; TIN, tumor infiltrating neutrophil; TIL, tumor infiltrating lymphocyte; GTC, giant tumor cell; CCC, clear cell carcinoma; EC, endometrioid carcinoma; SC, serous carcinoma; SEIC, serous intraepithelial carcinoma; *POLE*mut, DNA polymerase epsilon mutation; p53mut, p53 mutation; MMRd, mismatch repair-deficient; NSMP, no specific molecular profile; conv, conventional; LBC, liquid-based cytology; ca(+), adenocarcinoma; ca(s/o), AGC-favor neoplastic; AGC, atypical glandular cell; NILM, negative for intraepithelial lesion or malignancy; ne, no evaluation; na, not available; *FIGO Stage classification 2008.

Table II. *Distribution of clinical stage, tumor progression, and cytomorphometric features.*

Parameter	Classification	Molecular subtypes				Fisher's exact test			
		*POLE*mut	p53mut	MMRd	NSMP	MMRd *vs.* p53mut	NSMP *vs.* P53mut	NSMP *vs.* *POLE*mut	NSMP *vs.* MMRd
Stage	I+II	5	13	16	36	***p*=0.049**	***p*=0.008**	ns	ns
	III+IV	3	17	6	12				
pT category	pT1+pT2	8	19	17*	42	ns	***p*=0.022**	ns	ns
	pT3+pT4	0	11	4*	6				
Number of cytology specimens		8	28	22	45				
Abnormal cytology	None	2	11	10	18	ns	ns	ns	ns
	More than atypical cell	6	17	12	27				
Cell grouping	Large cluster	1	2	5	16	bs (*p*=0.092)	***p*=0.002**	bs (p=0.085)	ns
	Small cluster or single cell	5	15	7	11				
GCT	Present	3	9	3	2	ns	***p*=0.001**	***p*=0.031**	ns
	Absent	3	8	9	25				
TIN	Present	4	12	10	15	ns	ns	ns	ns
	Absent	2	5	2	12				
TIL	Present	5	8	9	7	ns	ns	***p*=0.016**	***p*=0.006**
	Absent	1	9	3	20				

*POLE*mut, DNA polymerase epsilon mutation; p53mut, p53 mutation; MMRd, mismatch repair-deficient; NSMP, no specific molecular profile; GCT, giant tumor cell; TIN, tumor infiltrating neutrophil; TIL, tumor infiltrating lymphocyte; ns, not significant; bs, borderline significance. *In each one case of MMRd- and NSMP-subtypes, no TNM information was obtained due to no operation. The frequencies in italics were compared *via* the Fisher's exact test. Bold values represent statistical significance.

GTCs were detected (Figure 2D). Although cSES was recognizable in conventional smear cytology specimens, the clusters were distorted, and cell detachment was less obvious than in the LBC specimens.

Cervical cytology of the other subtypes. The cytological features already mentioned were not specific to the *POLE*mut-subtype. Figure 3 presents the representative cytological findings for the other subtypes. In the p53mut-subtype, the tumor cells were arranged in small clusters or single cells (as observed in the *POLE*mut-subtype), exhibiting higher-grade nuclear atypia with occasional GTCs present (Figure 3A). These p53mut-subtype clusters exhibited cSES (Figure 3B) and included inflammatory cells. The MMRd-subtype exhibited large clusters containing TILs, TINs, or both (Figure 3C). The NSMP-subtype mostly appeared in large clusters, and cSES, TILs and TINs were less frequent than in the other subtypes (Figure 3D).

Quantitative comparison of cervical cytology. We performed quantitative analysis to extract cytomorphological features characteristic of the *POLE*mut-subtype to distinguish it from the NSMP-subtype. Abnormal cytology (AGC+AGC-favor neoplastic+adenocarcinoma) was most frequent in the *POLE*mut-subtype (75%), followed by the p53mut- (61%), NSMP- (60%), and MMRd- (55%) subtypes. However, the frequency of abnormal cytology was not considerably different among the 4 subtypes (Figure 4A, Table II). In contrast, cell grouping differed significantly among the four subtypes (Figure 4B). Specimens classified as having predominantly smaller clusters or single cells were more frequent in the p53mut-subtype than in the NSMP-subtype. The proportion of the different cell groupings exhibited borderline significant differences between the MMRd- and p53mut-subtypes (p=0.092) and between the *POLE*mut- and NSMP-subtypes (p=0.085) (Table II).

The *POLE*mut-subtype exhibited the highest frequency of atypical cell clusters with cSES (Figure 5A and B). ROC curve analysis revealed optimal cut-off value of 0.00 for the use of cSES frequency to distinguish the *POLE*mut-subtype from the other subtypes (Figure 5C), suggesting that the detection of even one cSES-positive cluster indicates a possible *POLE*mut-subtype diagnosis.

The frequency of GTC varied among the four subtypes (Figure 6A), being more frequent in the p53mut-subtype than in the NSMP-subtype. GTC frequency was significantly higher in the p53mut- and *POLE*mut-subtypes than in the NSMP-subtypes (Table II). TIN frequency was similar among the four subtypes (Figure 6B), whereas TIL frequency varied (Figure 6C). TIL frequency was significantly higher in the *POLE*mut- and MMRd-subtypes than in the NSNP-subtype (Table II). In summary, for the *POLE*mut-subtype,

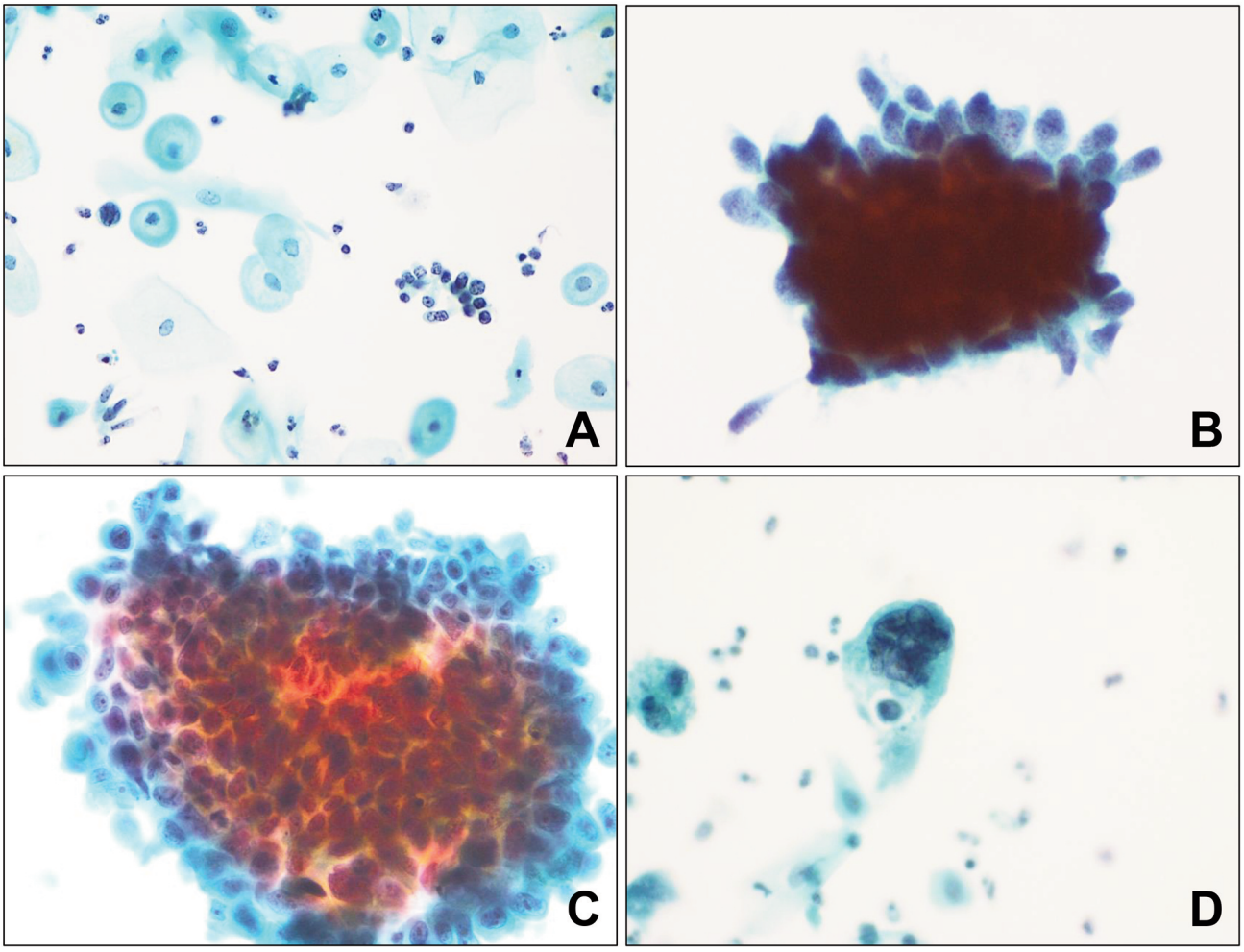

Figure 2. *Cytological features of POLEmut-subtype. (A) In the POLEmut-subtype, atypical cells occur frequently in small clusters or as single cells with moderate nuclear atypia (case 5). (B, C) Larger cell clusters exhibit partial (B) or complete cell dissociation at the perimeter (C), forming the cSES pattern (cases 7 and 5, respectively). Many of the clusters contain inflammatory cells (C). (D) Giant tumor cells are present in the atypical cells (case 6). Papanicolaou staining, ×40 magnification for scanning view (A) and ×400 magnification (B, C, D). POLEmut, DNA polymerase epsilon mutation.*

cervical cytology revealed frequent atypical cells with moderate nuclear atypia, in small clusters or as single cells, and with the presence of cSES and TILs. In contrast, the NSMP-subtype exhibited large clusters with less frequent cSES, TIL, and GTCs. Table III summarizes the representative cervical cytology features estimated *via* cytomorphological analyses of each subtype.

Discussion

Among the four subtypes, the *POLE*mut-subtype exhibited a higher incidence of abnormal cervical cytology in the form of cSES. Together with the presence of GTCs, cSES is suggestive of *POLE*mut subtype diagnosis (8, 9). Although an integrative diagnosis should be made using a combination of histology, IHC, and molecular examinations (9, 10), these findings reflect the usefulness of cervical cytology specimens in distinguishing the *POLE*mut-subtype from the NSMP-subtype.

In addition to glandular proliferation, endometrial cancers exhibit cellular features, such as mucin production, squamous metaplasia (morula) or obvious keratinization, clear cell changes, bizarre GTCs, and inflammatory cell infiltration into the cancer stroma and tumor nests (8, 15, 16). Endometrial cancers exhibit serous morphology, in which papillary growth generates a micropapillary pattern with hierarchical branching and condensation, leading to the formation of solid nests; this is diagnostic of serous carcinoma (4, 17, 18).

In contrast to serous morphology, SES occurs only in tumor cells facing the uterine lumen, and causes cell clusters to have more irregular contour, without hierarchical

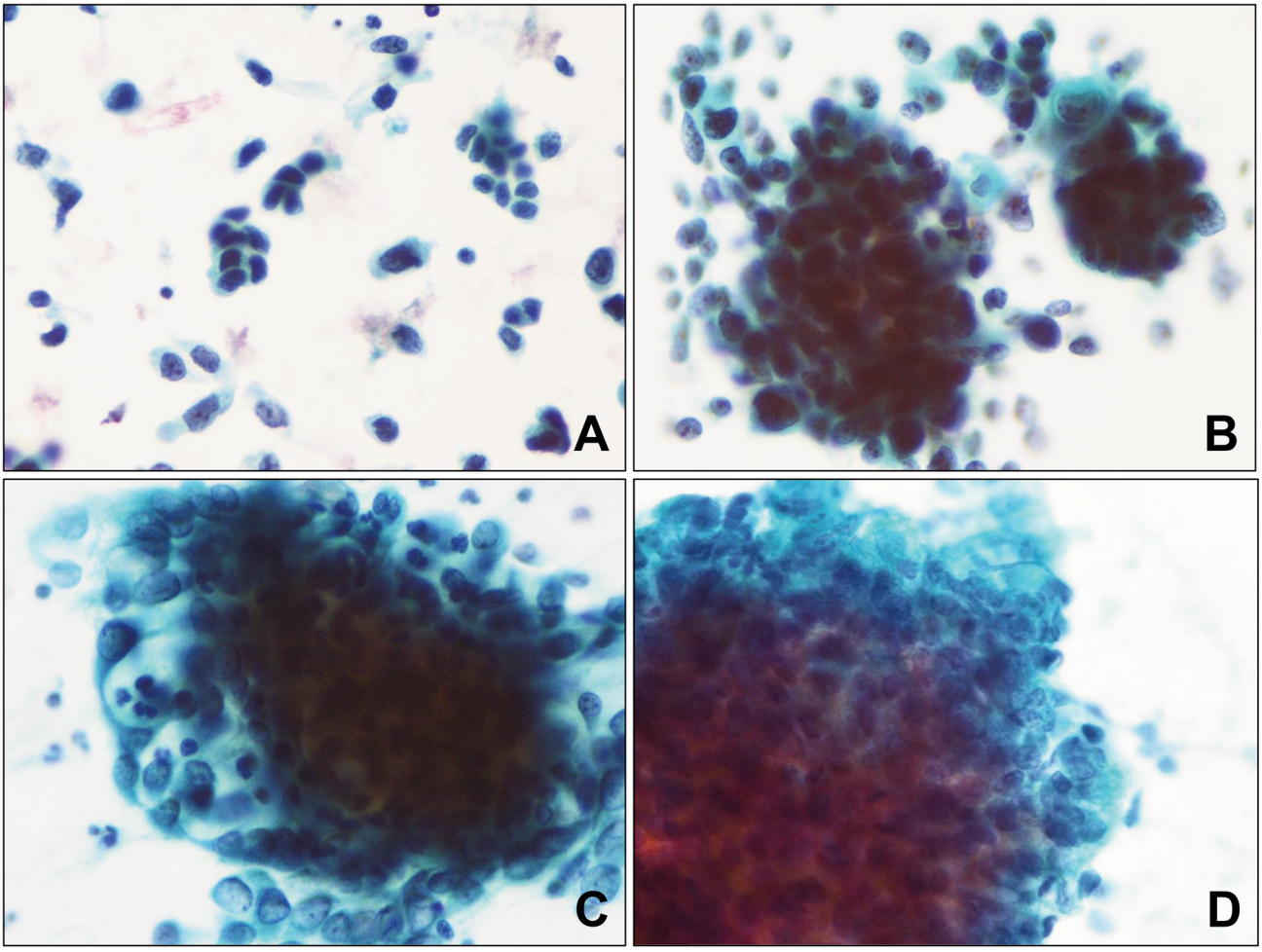

Figure 3. *Cytological features of the other subtypes. (A) In the p53mut-subtype, the atypical cells occur in small clusters or as single cells, with high-grade nuclear atypia; giant tumor cells are occasionally present (case 48). (B) The atypical cell clusters of the p53mut-subtype exhibit cSES (case 47). (C) In the MMRd-subtype, the atypical cells are present in large clusters that contain TILs, TINs, or both (case 16). (D) In the NSMP-subtype, the atypical cells occur in large clusters with low frequencies of cSES, TILs, and TINs (case 83). Papanicolaou staining, ×100 (A) and ×400 magnification (B, C, D). cSES: Cytologically detected surface epithelial slackening; MMRd: MMRd, Mismatch repair-deficient; TILs: tumor-infiltrating lymphocytes; TINs: tumor-infiltrating neutrophils; NSMP, no specific molecular profile; p53mut, p53 mutation.*

branching (9). In endometrioid carcinomas, SES-like papillary morphology has previously been referred to as "surface epithelial changes" (thin micropapillae without hierarchal branching) (19), or as small nonvillous papillae (20). These histological features may be reserved in cytological specimens, especially in LBC, which preserves cytomorphological features well (21, 22). Our findings reveal that the histologically detected SES morphology was well preserved in the cervical cytology specimens. Similarly, in our study, the histologically detected serous morphology of the p53mut-subtype was reflected in its cytomorphology, which revealed cSES-like cell dissociation from cell clusters. Consequently, we were unable to distinguish cytologically between SES and serous morphology. The cytomorphological detection of cSES involves cytological detection of serous morphology. Therefore, presumptive or differential cytological diagnosis of the *POLE*mut-subtype should be made *via* comprehensive cytological observation, and not only based on the detection of cSES.

In addition to the SES pattern, our detection of GTCs in cervical cytology corresponds to that previously reported using histological specimens (8, 9). Among the subtypes, TILs are observed predominantly in MMRd- and *POLE*mut-subtype histological and endometrial cytology specimens (8, 23), and TINs occur less frequently (9). Here, we found that the presence of TILs and TINs was preserved in cervical cytology. Therefore, these findings provide evidence that cervical cytology specimens can preserve not only the tumor

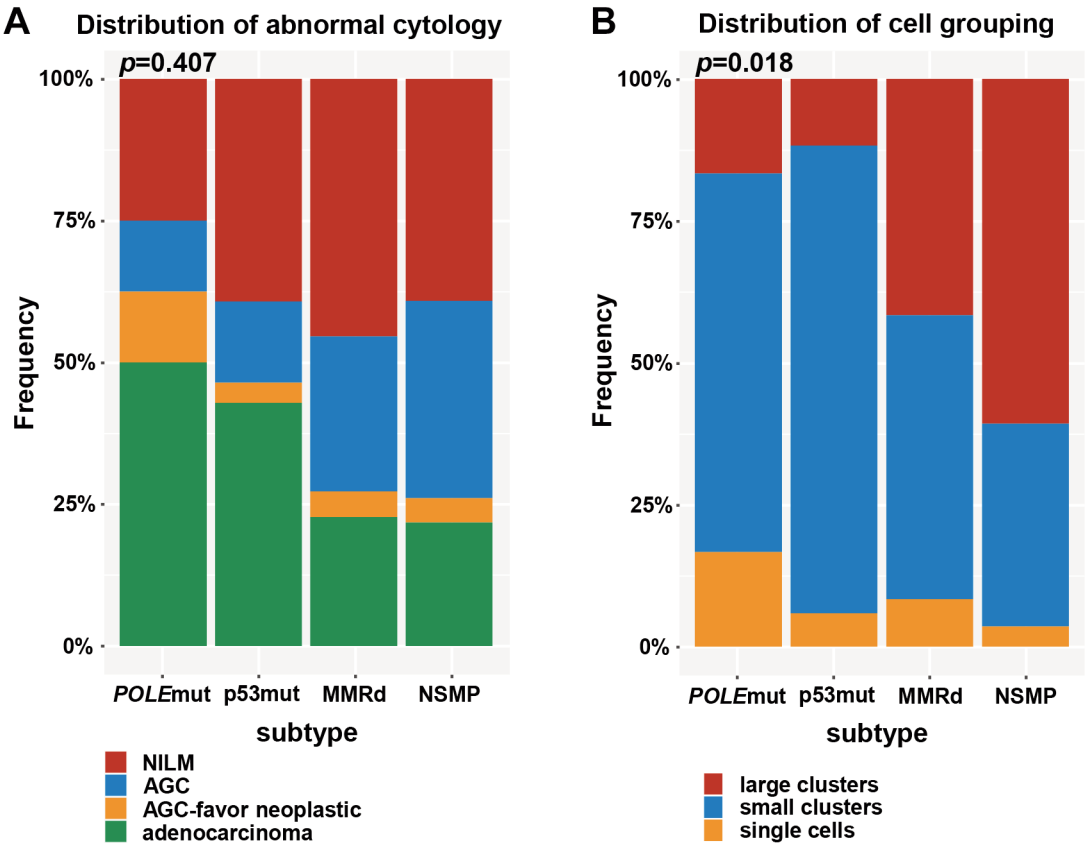

Figure 4. *Abnormal cytology and cell grouping in the four subtypes. (A) The frequency of abnormal cervical cytology (AGC + AGC-favor neoplastic + adenocarcinoma) is similar among the four subtypes. (B) In contrast, the cell grouping varies among the subtypes, with small clusters being more frequent in the p53mut- and POLEmut-subtypes (Table II). Differences among the four subtypes were evaluated using Fisher's exact test. MMRd, Mismatch repair-deficient; NSMP, no specific molecular profile; p53mut, p53 mutation; POLEmut, DNA polymerase epsilon mutation; AGC, atypical glandular cell.*

Table III. *Representative cytomorphology in each subtype of endometrial cancer.*

	Molecular subtypes			
Cytological features	*POLE*mut	p53mut	MMRd	NSMP
Nuclear atypia	Moderate to high	High	Moderate to high	Moderate to high
Cluster size	Small or single cell	Small or single cell	Large to small	Large
Cytological SES	Often	Occasional	Occasional	Rare
Giant tumor cell	Often	Often	Rare	Rare
TIN	Often	Often	Often	Often
TIL	Often	Occasional	Often	Rare

SES, Surface epithelial slackening; *POLE*mut, DNA polymerase epsilon mutation; p53mut, p53 mutation; MMRd, mismatch repair-deficient; NSMP, no specific molecular profile; GCT, giant tumor cell; TIN, tumor infiltrating neutrophil; TIL, tumor infiltrating lymphocyte.

cell structure or arrangement but also the tumor constituents detected in histological sections.

Endometrial cytology is not a popular procedure worldwide, whereas cervical cytology is a practical and less invasive screening tool for the detection of both cervical and endometrial cancers (24, 25). The reported frequencies of cervical cytology for the detection of endometrial cancers varies from 25.5% to 45.5% (26-29), while the non-

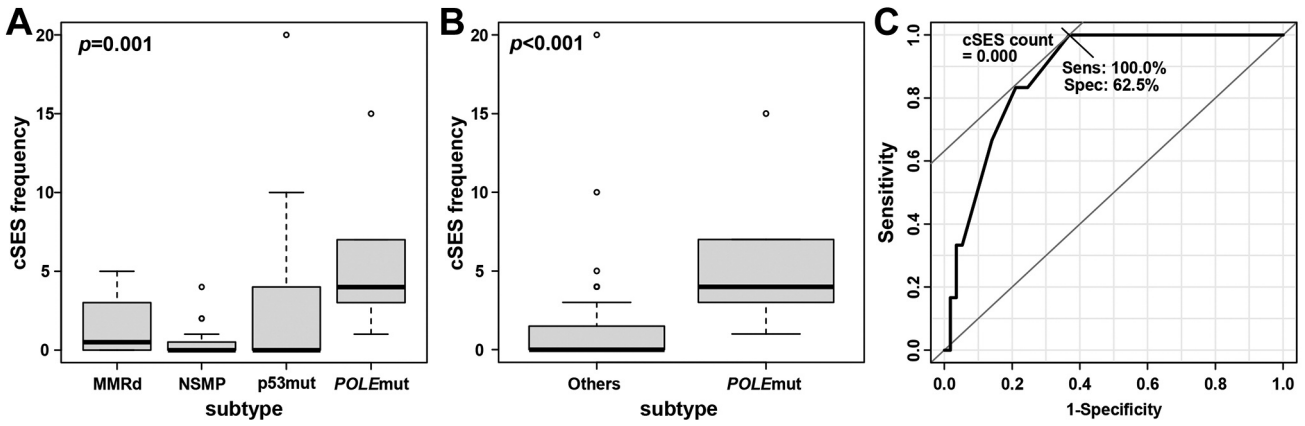

Figure 5. *SES frequency in atypical cell clusters. (A) Frequency of cSES in the four subtypes (Kruskal-Wallis test). (B) cSES frequency is significantly higher in the POLEmut-subtype than in the others (Wilcoxon test). (C) The receiver operator characteristic (ROC) curve reveals that the cut-off value of cSES frequency for distinguishing the POLEmut-subtype is 0.000, indicating that the presence of cSES is highly suggestive for the cytological diagnosis of POLEmut-subtype. SES, Surface epithelial slackening; cSES, cytologically detected SES; MMRd, mismatch repair-deficient; NSMP, no specific molecular profile; p53mut, p53 mutation; POLEmut, DNA polymerase epsilon mutation.*

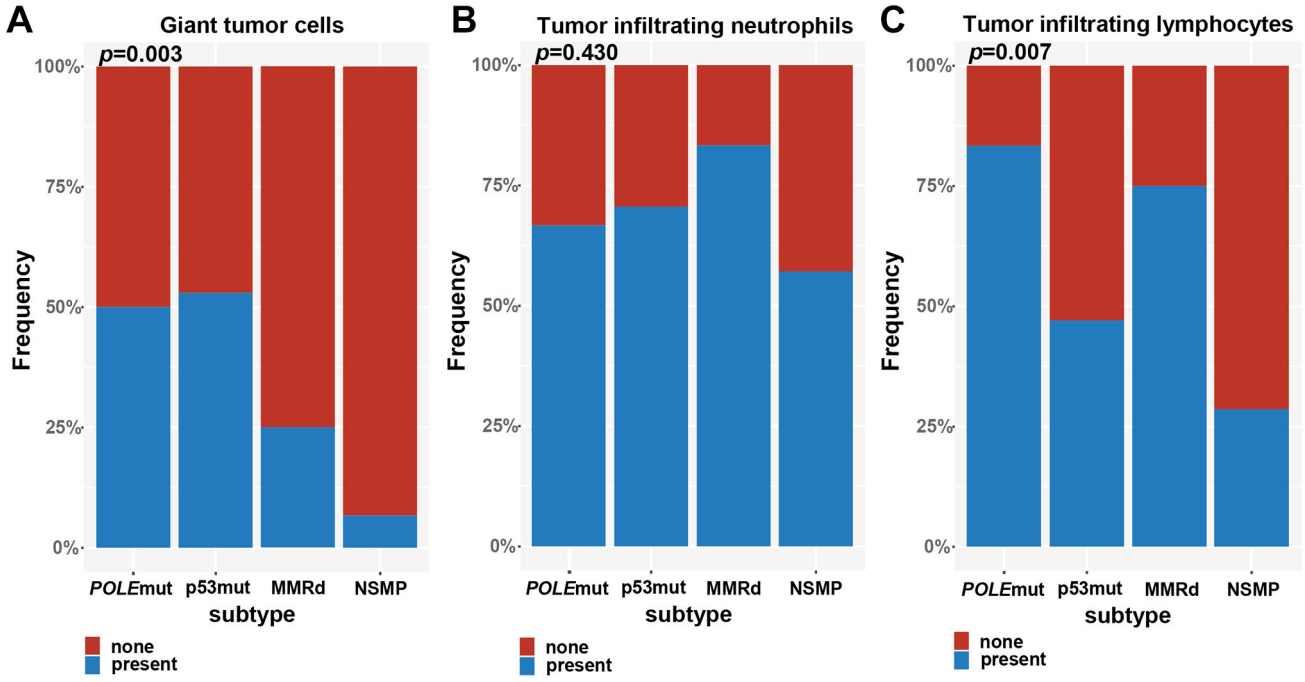

Figure 6. *GTC and tumor-infiltrating inflammatory cell frequency. (A) GTC frequency varies among the four subtypes, being higher in the p53mut- and POLEmut-subtypes. (B) Tumor-infiltrating neutrophils (TIN) frequency is similar among the four subtypes. (C) Tumor-infiltrating lymphocytes (TIL) frequency varies among the subtypes, being higher in the MMRd- and POLEmut-subtypes (Table II). The frequencies were compared via the Fisher's exact test. GTC: Giant tumor cells; MMRd, mismatch repair-deficient; NSMP, no specific molecular profile; p53mut, p53 mutation; POLEmut, DNA polymerase epsilon mutation.*

endometrioid subtype and serous carcinoma exhibit higher frequencies (77% and 65.7%, respectively) (26, 28). Consistent with this, in the present study, the frequency of abnormal cervical cytology was 60% (62/103 cases).

We have previously reported that a custom NGS cancer gene panel is useful for genomic classification of endometrial cancer according to the WHO system (10, 11). The approach of the WHO integrative diagnostic system,

which begins with genomic detection of the *POLE* mutation to differentiate the *POLE*mut-subtype (4, 6), might lead to incorrect molecular classification in cases with multiple-classifier phenotypes (30). The ProMisE system, which meets the minimal requirements of the WHO classification system (31), provides an alternative approach. This system begins with IHC to detect MMR, followed by hotspot Sanger sequencing of the *POLE* exonuclease domain, and loss of MMR expression is diagnostic of the MMRd-subtype (32). However, as with the WHO integrative diagnostic system, the ProMisE strategy can lead to misclassification in multiple-classifier phenotype cases, such as those with both MMR deficiency and the *POLE* mutation (30). Based on our findings, cytological detection of features such as cSES are suggestive of a possible *POLE*mut-subtype diagnosis and can help to prevent misclassification. Nonetheless, we recommend additional genomic examination *via* an NGS panel. These findings reveal that cervical cytological specimens provide an essential resource for integrative diagnosis in endometrial cancer. This approach is made easier by the fact that residual LBC specimens are widely available for use in molecular analyses including DNA-, RNA-, and methylation-based NGS analyses (33-37).

Conclusion

Our findings show that, in cervical cytology, the cSES pattern is unique to *POLE*mut-subtype endometrial cancer and occurs frequently in this subtype. Detection of cSES in cervical cytology specimens indicates a possible diagnosis of the *POLE*mut-subtype, although an integrative diagnosis including genomic profiling remains critical for diagnostic confirmation.

Availability of Data

The data supporting the findings of the study are available upon reasonable request from the corresponding author. The data are not publicly available due to privacy or ethical restrictions.

Conflicts of Interest

The Authors have no conflicts of interest to declare.

Authors' Contributions

Toshiaki Akahane, Emi Kubota, and Yukari Nishida-Kirita contributed as cytotechnologists; Toshiaki Akahane and Ikumi Kitazono analyzed and interpreted the sequencing data; Seiya Yokoyama performed statistical analyses; Ikumi Kitazono and Hirotsugu Noguchi contributed to cytopathological and histopathological diagnosis; Shintaro Yanazume and Miki Murakami summarized the clinical data; Hiroaki Kobayashi and Akihide Tanimoto organized the study design, and wrote the article; and all authors have read and approved the final manuscript.

Acknowledgements

We would like to thank Editage (www.editage.com) for English language editing.

References

1 Lappalainen T, Scott AJ, Brandt M, Hall IM: Genomic analysis in the age of human genome sequencing. Cell 177(1): 70-84, 2019. DOI: 10.1016/j.cell.2019.02.032

2 Holch JW, Metzeler KH, Jung A, Riedmann K, Jost PJ, Weichert W, Kirchner T, Heinemann V, Westphalen CB: Universal Genomic Testing: The next step in oncological decision-making or a dead end street? Eur J Cancer 82: 72-79, 2017. DOI: 10.1016/j.ejca.2017.05.034

3 Horak P, Fröhling S, Glimm H: Integrating next-generation sequencing into clinical oncology: strategies, promises and pitfalls. ESMO Open 1(5): e000094, 2016. DOI: 10.1136/esmoopen-2016-000094

4 Kim KR, Lax SF, Lazar AJ, Longacre TA, Malpica A, Matias-Guiu X, Nucci MR, Oliva E: Tumours of the uterine corpus. In: WHO classification of tumours female genital tumours, 5th edition. Lyon, France, IARC, pp. 245-308, 2020.

5 Cancer Genome Atlas Research Network, Kandoth C, Schultz N, Cherniack AD, Akbani R, Liu Y, Shen H, Robertson AG, Pashtan I, Shen R, Benz CC, Yau C, Laird PW, Ding L, Zhang W, Mills GB, Kucherlapati R, Mardis ER, Levine DA: Integrated genomic characterization of endometrial carcinoma. Nature 497(7447): 67-73, 2013. DOI: 10.1038/nature12113

6 Vermij L, Smit V, Nout R, Bosse T: Incorporation of molecular characteristics into endometrial cancer management. Histopathology 76(1): 52-63, 2020. DOI: 10.1111/his.14015

7 Kitazono I, Kobayashi Y, Akahane T, Yamaguchi T, Yanazume S, Nohara S, Sakamoto I, Tabata K, Tasaki T, Kobayashi H, Tanimoto A: ATM immunohistochemistry as a potential marker for the differential diagnosis of no specific molecular profile subtype and POLE-mutation subtype endometrioid carcinoma. Pathol Res Pract 230: 153743, 2022. DOI: 10.1016/j.prp.2021.153743

8 Van Gool IC, Ubachs JEH, Stelloo E, de Kroon CD, Goeman JJ, Smit VTHBM, Creutzberg CL, Bosse T: Blinded histopathological characterisation of POLE exonuclease domain-mutant endometrial cancers: sheep in wolf's clothing. Histopathology 72(2): 248-258, 2018. DOI: 10.1111/his.13338

9 Kitazono I, Akahane T, Yokoyama S, Kobayashi Y, Togami S, Yanazume S, Tasaki T, Noguchi H, Tabata K, Kobayashi H, Tanimoto A: "Surface epithelial slackening" pattern in endometrioid carcinoma: A morphological feature for differentiating the POLE mutation-subtype from the no specific molecular profile subtype. Pathol Res Pract 247: 154563, 2023. DOI: 10.1016/j.prp.2023.154563

10 Kobayashi Y, Kitazono I, Akahane T, Yanazume S, Kamio M, Togami S, Nohara S, Sakamoto I, Yokoyama S, Tabata K, Kobayashi H, Tanimoto A: Molecular evaluation of endometrial dedifferentiated carcinoma, endometrioid carcinoma, carcinosarcoma, and serous carcinoma using a custom-made small cancer panel. Pathol Oncol Res 27: 1610013, 2021. DOI: 10.3389/pore.2021.1610013

11 Akahane T, Kitazono I, Yanazume S, Kamio M, Togami S, Sakamoto I, Nohara S, Yokoyama S, Kobayashi H, Hiraki T,

Suzuki S, Ueno S, Tanimoto A: Next-generation sequencing analysis of endometrial screening liquid-based cytology specimens: a comparative study to tissue specimens. BMC Med Genomics 13(1): 101, 2020. DOI: 10.1186/s12920-020-00753-6

12 Xu C, Gu X, Padmanabhan R, Wu Z, Peng Q, DiCarlo J, Wang Y: smCounter2: an accurate low-frequency variant caller for targeted sequencing data with unique molecular identifiers. Bioinformatics 35(8): 1299-1309, 2019. DOI: 10.1093/bioinformatics/bty790

13 Brierley JD, Gospodarowicz MK, Wittekind C: Gynaecological tumours: TNM classification of malignant tumours, eighth edition. Oxford, UK, Wiley Blackwell, pp. 171-174, 2017.

14 Wilbur DC, Chhieng DC, Guidos B, Mody DR: Epithelial abnormalities: Glandular. The Bethesda System for Reporting Cervical Cytology: 193-240, 2015. DOI: 10.1007/978-3-319-11074-5_6

15 Murali R, Davidson B, Fadare O, Carlson JA, Crum CP, Gilks CB, Irving JA, Malpica A, Matias-Guiu X, McCluggage WG, Mittal K, Oliva E, Parkash V, Rutgers JKL, Staats PN, Stewart CJR, Tornos C, Soslow RA: High-grade endometrial carcinomas: Morphologic and immunohistochemical features, diagnostic challenges and recommendations. Int J Gynecol Pathol 38 Suppl 1(Iss 1 Suppl 1): S40-S63, 2019. DOI: 10.1097/PGP.0000000000000491

16 Lucas E, Carrick KS: Low grade endometrial endometrioid adenocarcinoma: A review and update with emphasis on morphologic variants, mimics, immunohistochemical and molecular features. Semin Diagn Pathol 39(3): 159-175, 2022. DOI: 10.1053/j.semdp.2022.02.002

17 Wei JJ, Paintal A, Keh P: Histologic and immunohistochemical analyses of endometrial carcinomas: experiences from endometrial biopsies in 358 consultation cases. Arch Pathol Lab Med 137(11): 1574-1583, 2013. DOI: 10.5858/arpa.2012-0445-OA

18 Hoang LN, McConechy MK, Köbel M, Han G, Rouzbahman M, Davidson B, Irving J, Ali RH, Leung S, Mcalpine JN, Oliva E, Nucci MR, Soslow RA, Huntsman DG, Gilks CB, Lee C: Histotype-genotype correlation in 36 high-grade endometrial carcinomas. Am J Surg Pathol 37(9): 1421-1432, 2013. DOI: 10.1097/PAS.0b013e31828c63ed

19 Singh K, Simon RA, Zhang C, Quddus MR: "Surface epithelial changes" in uterine endometrioid carcinoma mimicking micropapillary serous borderline tumor of ovary: report of two cases and review of the literature. Diagn Pathol 6: 13, 2011. DOI: 10.1186/1746-1596-6-13

20 Murray SK, Young RH, Scully RE: Uterine endometrioid carcinoma with small nonvillous papillae: an analysis of 26 cases of a favorable-prognosis tumor to be distinguished from serous carcinoma. Int J Surg Pathol 8(4): 279-289, 2000. DOI: 10.1177/106689690000800407

21 Tanaka R, Fujiwara M, Sakamoto N, Kanno H, Arai N, Tachibana K, Kishimoto K, Anraku M, Shibahara J, Kondo H: Cytological characteristics of histological types of lung cancer by cytomorphometric and flow cytometric analyses using liquid-based cytology materials. Diagn Cytopathol 51(6): 356-364, 2023. DOI: 10.1002/dc.25118

22 Tanaka R, Fujiwara M, Sakamoto N, Suzuki H, Tachibana K, Ohtsuka K, Kishimoto K, Kamma H, Shibahara J, Kondo H: Cytomorphometric and flow cytometric analyses using liquid-based cytology materials in subtypes of lung adenocarcinoma. Diagn Cytopathol 50(8): 394-403, 2022. DOI: 10.1002/dc.24978

23 Yanazume S, Iwakiri K, Kobayashi Y, Kitazono I, Akahane T, Mizuno M, Togami S, Tanimoto A, Kobayashi H: Cytopathological features associated with *POLE* mutation in endometrial cancer. Cytopathology 34(3): 211-218, 2023. DOI: 10.1111/cyt.13215

24 Munakata S: Diagnostic value of endometrial cytology and related technology. Diagn Cytopathol 50(7): 363-366, 2022. DOI: 10.1002/dc.24956

25 Toyoda S, Kawaguchi R, Kobayashi H: Clinicopathological characteristics of atypical glandular cells determined by cervical cytology in Japan: Survey of gynecologic oncology data from the Obstetrical Gynecological Society of Kinki District, Japan. Acta Cytol 63(5): 361-370, 2019. DOI: 10.1159/000498977

26 Skaznik-wikiel ME, Ueda SM, Frasure HE, Rose PG, Fleury A, Grumbine FC, Fader AN: Abnormal cervical cytology in the diagnosis of uterine papillary serous carcinoma: earlier detection of a poor prognostic cancer subtype. Acta Cytologica 55(3): 255-260, 2011. DOI: 10.1159/000324052

27 Amkreutz LCM, Pijnenborg JMA, Joosten DWL, Mertens HJMM, Van Kuijk SMJ, Engelen MJA, Bergmans M, Nolting WE, Kruitwagen RFPM: Contribution of cervical cytology in the diagnostic work-up of patients with endometrial cancer. Cytopathology 29(1): 63-70, 2018. DOI: 10.1111/cyt.12511

28 Frias-Gomez J, Benavente Y, Ponce J, Brunet J, Ibáñez R, Peremiquel-Trillas P, Baixeras N, Zanca A, Piulats JM, Aytés Á, Matias-Guiu X, Bosch FX, de Sanjosé S, Alemany L, Costas L, Screenwide Team: Sensitivity of cervico-vaginal cytology in endometrial carcinoma: a systematic review and meta-analysis. Cancer Cytopathol 128(11): 792-802, 2020. DOI: 10.1002/cncy.22266

29 Frias-Gomez J, Tovar E, Vidal A, Murgui L, Ibáñez R, Peremiquel-Trillas P, Paytubi S, Baixeras N, Zanca A, Ponce J, Pineda M, Brunet J, de Sanjosé S, Bosch FX, Matias-Guiu X, Alemany L, Costas L, Screenwide Team: Sensitivity of cervical cytology in endometrial cancer detection in a tertiary hospital in Spain. Cancer Med 10(19): 6762-6766, 2021. DOI: 10.1002/cam4.4217

30 León-Castillo A, Gilvazquez E, Nout R, Smit VT, McAlpine JN, McConechy M, Kommoss S, Brucker SY, Carlson JW, Epstein E, Rau TT, Soslow RA, Ganesan R, Matias-Guiu X, Oliva E, Harrison BT, Church DN, Gilks CB, Bosse T: Clinicopathological and molecular characterisation of 'multiple-classifier' endometrial carcinomas. J Pathol 250(3): 312-322, 2020. DOI: 10.1002/path.5373

31 Kommoss S, McConechy MK, Kommoss F, Leung S, Bunz A, Magrill J, Britton H, Kommoss F, Grevenkamp F, Karnezis A, Yang W, Lum A, Krämer B, Taran F, Staebler A, Lax S, Brucker SY, Huntsman DG, Gilks CB, McAlpine JN, Talhouk A: Final validation of the ProMisE molecular classifier for endometrial carcinoma in a large population-based case series. Ann Oncol 29(5): 1180-1188, 2018. DOI: 10.1093/annonc/mdy058

32 Talhouk A, McConechy MK, Leung S, Yang W, Lum A, Senz J, Boyd N, Pike J, Anglesio M, Kwon JS, Karnezis AN, Huntsman DG, Gilks CB, McAlpine JN: Confirmation of ProMisE: A simple, genomics-based clinical classifier for endometrial cancer. Cancer 123(5): 802-813, 2017. DOI: 10.1002/cncr.30496

33 Akahane T, Yamaguchi T, Kato Y, Yokoyama S, Hamada T, Nishida Y, Higashi M, Nishihara H, Suzuki S, Ueno S, Tanimoto A: Comprehensive validation of liquid-based cytology specimens for next-generation sequencing in cancer genome

analysis. PLoS One 14(6): e0217724, 2019. DOI: 10.1371/journal.pone.0217724
34 Yamaguchi T, Akahane T, Harada O, Kato Y, Aimono E, Takei H, Tasaki T, Noguchi H, Nishihara H, Kamata H, Tanimoto A: Next-generation sequencing in residual liquid-based cytology specimens for cancer genome analysis. Diagn Cytopathol 48(11): 965-971, 2020. DOI: 10.1002/dc.24511
35 Akahane T, Kitazono I, Kobayashi Y, Nishida-Kirita Y, Yamaguchi T, Yanazume S, Tabata K, Kobayashi H, Tanimoto A: Direct next-generation sequencing analysis using endometrial liquid-based cytology specimens for rapid cancer genomic profiling. Diagn Cytopathol 49(9): 1078-1085, 2021. DOI: 10.1002/dc.24841
36 Yokoyama S, Iwaya H, Akahane T, Hamada T, Higashi M, Hashimoto S, Tanoue S, Ohtsuka T, Ido A, Tanimoto A: Sequential evaluation of MUC promoter methylation using next-generation sequencing-based custom-made panels in liquid-based cytology specimens of pancreatic cancer. Diagn Cytopathol 50(11): 499-507, 2022. DOI: 10.1002/dc.25022
37 Akahane T, Isochi-Yamaguchi T, Hashiba-Ohnuki N, Bandoh N, Aimono E, Kato Y, Nishihara H, Kamada H, Tanimoto A: Cancer gene analysis of liquid-based cytology specimens using next-generation sequencing: A technical report of bimodal DNA- and RNA-based panel application. Diagn Cytopathol 51(8): 493-500, 2023. DOI: 10.1002/dc.25149

Received September 23, 2023
Revised October 28, 2023
Accepted October 31, 2023